

Design of the Main Nozzle with Different Acceleration Tube and Diameter in an Air-Jet Loom

Seok-Yoon Jeong¹, Kyung-Hoon Kim^{#,1}, Jin-Hwan Choi¹, Chan-kyu Lee²

¹ School of Mechanical Engineering, KyungHee University, Suwon, South Korea

² Dept. of Mechanical Engineering, Koje College

ABSTRACT

The air-jet loom represents a major step in the development of shutterless weaving due to its ability to weave a wide range of yarns at high speeds. The air-jet weaving involves inserting a pre-measured length of yarn through the wraps, which is shed by means of compressed air. The analysis of air flow characteristic of the main nozzle and acceleration tube is required for improving the loom performance. In this paper, we examined the effects of the main nozzle with different acceleration tubes as well as diameters. Also, we compared the performance of a straight-type tube with a Laval-type tube and the effect of installing a suction hole on the acceleration tube.

Key Words: Nozzle, Air-Jet Loom, Air-jet weaving, Acceleration Tube, Shutterless weaving

1. Introduction

Recently, lots of studies on the air-jet loom using high-pressure air have been carried on due to its advantages such as high productivity, widespread weaving, excellent quality of textile fabrics, convenient operation, the least pollution via using the atmospheric air, and the feasibility of automation. However, many technical problems are emerging as the studies go on. In particular, of considerable importance is how to design the main nozzle which, due to overconsuming high-pressure air, causes noise and vibration as well as lowers economical efficiency. The most serious problem concerning the air-jet loom is how to make the yarn flight as far and exactly as possible with desirable efficiency.¹ For this purpose, the flow characteristics in the main nozzle should be fully understood.² However,

despite a lot of available experimental results,³ further studies are required due to lack of precision instruments and meaningful data up to date. Therefore the purpose of this study is to design the optimum nozzle by comparing and considering the results of the studies^{4~7} from the past; the inner diameter change of acceleration tube, straight-tube type pipe and Laval-tube type pipe. Also, it is aimed at analyzing through examining and measuring the effects of the existence of the suction hole and the flow distribution at the exit of the acceleration tube.

2. Experiment

2.1 Experiment systems

2.1.1 Air-jet pressure control system

As shown in Fig. 1, the air pressure from the compressor, which serves as the air source, passes through several devices (air filter, air tank, pressure controller, pressure gauge, and straight-type flow meter) and is finally guided to the main nozzle. The flow is

Manuscript received: October 29, 2003;

Accepted: June 30, 2004

Corresponding Author :

E-mail : kimkh@khu.ac.kr

Tel.: +82-31-201-2509, Fax : +82-31-202-8106

made to be steady-state at a proper time interval by setting the solenoid valve to avoid an intermittent flow.

2.1.2 Nozzle, needle and acceleration tube

The main nozzle consists of three parts as shown in Fig. 2; nozzle body, needle and acceleration tube.

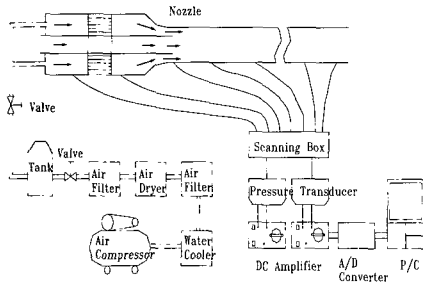


Fig. 1 Schematic outline of experimental apparatus

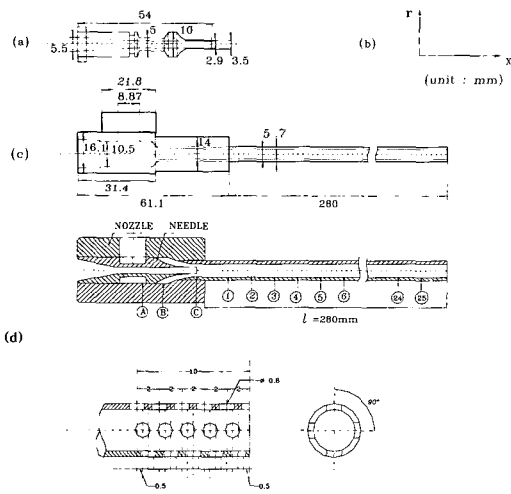


Fig. 2 Configuration and dimension of main nozzle
 (a) needle part of the main nozzle,
 (b) nozzle body and acceleration tube,
 (c) main nozzle,
 (d) enlarged picture of the drilled hole to measure the air pressure in the acceleration tube.

The needle has a weft passage in its center, and its thin-tapered head is inserted into the nozzle body. The compressed air from the needle body (C in Fig. 2(c)) flows, from the first air-gathering part (A), through the outer periphery of the needle. Then, after passing

through the commutators that are radially placed on the outer surface of the needle and passing through the second air-gathering part (B), the compressed air continues to flow around the taper. The cross-sectional area of the flow passage around the taper decreases toward the needle tip.

Thereafter, the flow passage is sharply expanded because the air flow is connected to the acceleration tube. The flow in the acceleration tube is characterized to be the Fanno flow, which is a constant diameter tube, and is finally discharged to the atmosphere at the exit of the acceleration tube.

Each part of the main nozzle, shown in Fig. 2, has the following configuration: $d_o = 3.5$ mm (the external diameter of needle tip), $d_i = 2.9$ mm (the internal diameter of needle tip), $D = 4$ mm (the inner diameter of acceleration tube), and $L = 280$ mm (the length of acceleration tube). Also an additional needle tip is separately designed and manufactured in order to alter the inner diameter of the acceleration tube, for example, to make $D = 3$ mm.

2.2 Experimental methods

To analyze the flow in the main nozzle shown in Fig. 2(c), each hole, which is 0.8 mm in diameter and measures the static pressure, is set up individually in the first and second air-gathering parts of the main nozzle and in the needle tip.

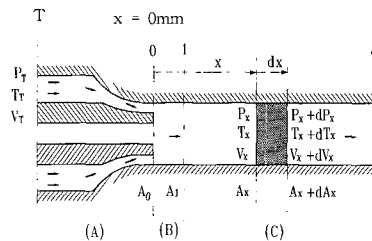


Fig. 3 Classification of flow in main nozzle

Also, in the acceleration tube, which is attached to the main nozzle body, the static-pressure measuring hole of $\phi = 0.8$ mm is set up to measure the static pressure on the wall surface. When the needle tip is selected to be the origin (i.e. $x = 0$ mm) for ease of understanding, the measuring holes are distributed at $x = -21$ mm (the first air-gathering part), $x = -13$ mm (the

air-gathering part), and also at 24 places in the acceleration tube with 10 mm interval starting from $x = 15$ mm (position ① in Fig. 2(c)) up to $x = 245$ mm. However, all the holes except certain measuring holes are shut during the measurement of the pressure.

3. Flow analysis according to range in the Nozzle

The main nozzle plays an important role that selects the weft for the loom in the beginning and then inserts it into the warp threads. The main nozzle is linked with the acceleration tube from the air insertion part of the nozzle body (the first air-gathering part), the tapered passage part of the needle (the second air-gathering part) and the minimum cross-sectional area of the needle tip.

To analyze the flow in the main nozzle, we can consider three different regions, as shown in Fig. 3. Region A is the outer wall of the nozzle, from the inner nozzle body to the needle tip and the tapered loop passage surrounding the needle. In Region A, the flow is the reduced nozzle flow. Next, Region B is from the needle tip where the loop flow suddenly expands to the entrance of the acceleration tube, where the flow becomes uniform after mixing with a suction flow from the yarn passage of the needle. The flow in Region B is the sudden expansion tube flow. Lastly, Region C is from the entrance of the acceleration tube where the flow is uniformly mixed to the exit. The cross section is constant and friction occurs at the tube wall. In Region C, the flow is the Fanno flow which is adiabatic.

3.1 Flow of the region A

- The flow in the contract nozzle

The contract nozzle or the converging nozzle, is the one that has a minimum cross section at the exit where the cross section slowly decreases according to the drift of flow. Under the circumstance that the air tank is at a static condition, according to the change in P_T , which is the supply pressure of the nozzle, the flow speed at the exit of the contract nozzle (i.e. the needle tip) reaches the sonic speed. In such a case, we call the fractional pressure as the critical pressure P^* , then the flow in the contract nozzle can be largely analyzed into three sections.

If the supply pressure P_T slowly rises, the pressure at the throat is higher than the pressure P^* of the critical point where the flow speed at the throat becomes the sonic speed. In this case, the flow in the nozzle becomes subsonic overall, and the corresponding mass flow, which can be predicted from the subsonic isentropic flow, is smaller than the critical value. However, if the supply pressure P_T is exactly the same as the critical pressure P^* , the flows at the throat and the nozzle exit are sonic and the mass flow becomes a maximum value. Concomitantly, the throat upstream is a subsonic flow and can be analyzed by the isentropic flow based on the local area ratio. Lastly, if the supply pressure P_T is higher than the critical pressure P^* , the nozzle cannot respond any longer because it is choked when maximum mass flow occurs in the throat. In this case, the pressure at the throat is P^* and the flow remains at the sonic speed. Also, the distribution of the nozzle pressure is the same as the one corresponding to the critical pressure P^* . For the supersonic jet at the exit, any change to influence the choked flow condition of the nozzle cannot be sent to the upstream.

The flow at cross section 0 is changed by the ratio of the pressure P_T , at cross section T shown in Fig. 3 and the pressure P_0 , at cross section 0. Hence the total quantity at cross section 0 can be obtained according to each condition.

The flow at cross section 0 is at a subsonic speed or at a critical condition of $M_0 = 1$. In case of a subsonic speed, $P_0 = P_1$, thus the energy equation becomes as follows:

$$h_0 + \frac{V_0^2}{2} = h_T + \frac{V_T^2}{2} \quad (1)$$

Here, the flow speed V_0 at cross section 0 can be obtained from the pressure P_T at the congested point, as well as the temperature T_T and the pressure $P_1 (= P_0)$ at the entrance of the acceleration tube.

$$\frac{P_T}{P_0} = \left(1 + \frac{k-1}{2} M_0^2\right)^{k/(k-1)} \quad (2)$$

We can get the Mach number M_0 from the above equation, and the flow rate from the following equations

$$T_0 = T_T / (1 + \frac{k-1}{2} M_0^2) \quad (3)$$

$$\rho_0 = \rho_T / (1 + \frac{k-1}{2} M_0^2)^{1/(k-1)} \quad (4)$$

$$C_0 = \sqrt{k R T_0} \quad (5)$$

When the flow at cross section 0 is at a critical condition, we impose the condition $M_0 = 1$ and can apply the above equation again.

3.2 Flow characteristics in region B

- The flow in the sudden divergent nozzle

The jet from the needle tip is located at the sudden expanded tube passage at the exit of the acceleration tube and the flow abruptly expands at this region. In the nozzle used in this experiment, the extension tube ratio, which is the ratio of the external diameter of the minimum cross section (Slot port) at the needle tip and the inner diameter of the acceleration tube, is rather small. Therefore, when the slot port of the needle is in the subsonic region, the pressure P_0 at cross section 0 of the slot port shown in Fig. 3 can be assumed to be the same as the measured pressure P_1 at cross section 1 where the flow is uniform at the entrance of the acceleration tube. Also, when the slot port of the needle is in the sonic region, the flow rate is computed as if P_0 is the critical pressure.

The basic equations in the inspection volume between cross section 0 and 1 are as follows.

$$\rho_0 V_0 A_0 = \rho_1 V_1 A_1 = \dot{m} \quad (6)$$

$$\int_0^1 \frac{dP}{\rho} + \frac{V_1^2}{2} = \frac{V_0^2}{2} \quad (7)$$

$$h_0 + \frac{V_0^2}{2} = h_1 + \frac{V_1^2}{2} \quad \text{or}$$

$$\frac{C_0^2}{k-1} + \frac{V_0^2}{2} = \frac{C_1^2}{k-1} + \frac{V_1^2}{2} \quad (8)$$

$$\frac{P_1}{P_0} = \frac{A_0 M_0}{A_1 M_1} \sqrt{\frac{2 + (k-1)M_0^2}{2 + (k-1)M_1^2}} \quad (9)$$

The Mach number M_1 can be determined from the above equation by substituting the cross sectional area A_0, A_1 (at cross section 0, 1), the flow quantity M_0, P_0 (at cross section 0) obtained from the aforementioned equations, and the static pressure P_1 at the wall surface of cross-section 1. Using the Mach number M_1 , the flow quantities at cross section 1 can be calculated from the following equations:

$$V_1 = \sqrt{k R T_1} \quad (10)$$

$$T_1 = T_0 \cdot \frac{(1 + \frac{k-1}{2} M_0^2)}{(1 + \frac{k-1}{2} M_1^2)} \quad (11)$$

$$\rho_1 = \frac{P_1}{R T_1} \quad (12)$$

3.3 Flow characteristics in region C

- Fanno flow

The flow characteristics in the acceleration tube are analyzed by the Fanno flow which occurs at the constant cross-section region with friction but no heat transfer with the surrounding. The flow in the nozzle is assumed to be isentropic. For the Fanno flow occurring in constant cross-section passage and for the constant back pressure, the pressure change according to the flow distance X depends on the pressure at the nozzle exit.

After the pressure at the nozzle exit increases to a certain limit as high as the critical pressure, pressures at the nozzle and fluid passage decrease all together. If the pressure at the nozzle exit is equal to the critical pressure, the Mach number is 1 at the exit of the acceleration tube. Unless the flow condition in the nozzle and the duct are changed, further increase in the pressure at the nozzle exit higher than the critical pressure cannot alter the mass flow since the flow is already choked (i.e. the flow at the nozzle exit is at the sonic speed). Such an increase in the Mach number is primarily due to the reduction of the efficient cross section in the flow passage by the development of the boundary layer by friction of the tube at the wall surface along the flow direction.

The basic equations for the Fanno flow are as follows:

$$\rho dV + V d\rho = 0 \quad (13)$$

$$-\frac{dF_f}{A} - dP = \rho V dV \quad \text{or}$$

$$dP + \rho V dV = -\left(\frac{f dx}{D_H}\right) \frac{1}{2} \rho V^2 \quad (14)$$

$$dh + d\left(\frac{V^2}{2}\right) = 0 \quad (15)$$

The effect of friction acting over two cross sections can be described by the following equation:

$$\frac{f}{D_H} dx = \frac{2}{kM^2} \frac{1-M^2}{1+\frac{k-1}{2}M^2} \frac{dM}{M} \quad (16)$$

If the distance from an arbitrary cross-section, where the Mach number is M , to the sonic cross-section (where $M=1$) is denoted by L^* , Eq. (16) could be rewritten such that

$$\frac{fL^*}{D_H} = \frac{1-M^2}{kM^2} + \frac{k+1}{2k} \ln\left[\frac{(k+1)M^2}{2+(k-1)M^2}\right] \quad (17)$$

By selecting the standard condition to be the critical condition, and by denoting flow quantities at the critical condition P^* , ρ^* , and T^* , the flow conditions at any arbitrary cross section can be described using the Mach number as follows

$$\frac{T}{T^*} = \frac{k+1}{2+(k-1)M^2} \quad (18)$$

$$\frac{P}{P^*} = \frac{1}{M} \left[\frac{k+1}{2+(k-1)M^2} \right]^{1/2} \quad (19)$$

$$\frac{\rho}{\rho^*} = \frac{1}{M} \left[\frac{2+(k-1)M^2}{k+1} \right]^{1/2} \quad (20)$$

From the above equations, we can get the Mach number at any cross-section x .

4. Result and Discussion

4.1 The analysis and comparison of the flow by change of acceleration tube's inner diameter

4.1.1 The flow analysis at diameter of 4mm

For the case of $P_T = 5 \text{ kg}_f/\text{cm}^2$ at which the Fanno flow is settled, the flow corresponding to $D_i = 4 \text{ mm}$ gives the critical distance $L^* = 195.67 \text{ mm}$, as shown in Fig. 5 and Fig. 4. It can be seen from Fig. 5 that the Mach number slowly increases for the Fanno flow region in the acceleration tube. As a result, the Mach number M attains its maximum at the exit of the acceleration tube and choking takes place at the point of critical distance.

Under this condition, however, several nuisances occur such as overconsumption of compressed air and the lack of driving of weft and driving force. When compared with the state-of-the-art products, this reveals that the meaning of the critical distance fades away unless $D_i = 4 \text{ mm}$ is the optimal size. Thus, it would be better not to enlarge P_T as much as possible, and the critical distance should be sought for a range of $P_T (5 \text{ kg}_f/\text{cm}^2)^2$.

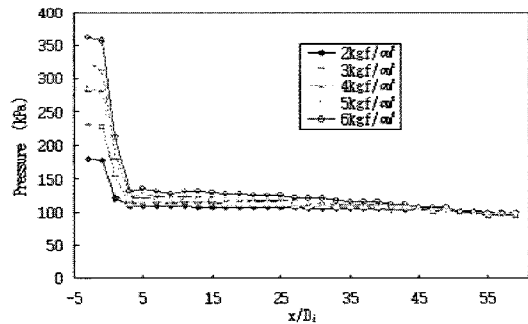


Fig. 4 Distribution of static pressure on wall surface along x -axis ($D_i = 4 \text{ mm}$)

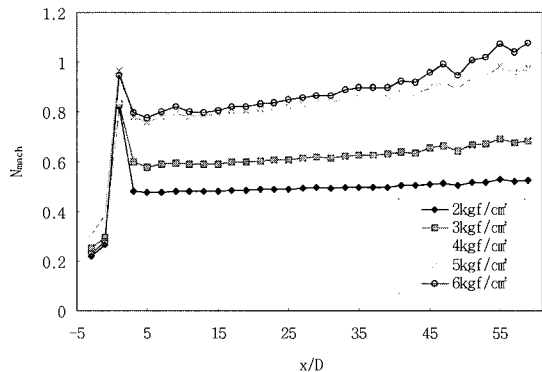


Fig. 5 Distribution of Mach number along x -axis ($D_i = 4 \text{ mm}$)

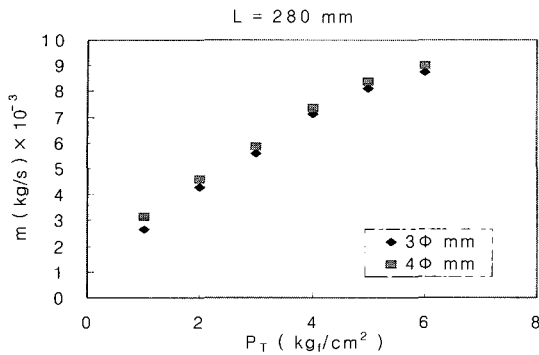


Fig. 6 Distribution of mass flow rate

4.1.2 Flow analysis at 3mm diameter

For the acceleration tube of $D_i=3\text{mm}$ rather than $D_i=4\text{mm}$, the nuisances are alleviated a little. For example, overconsumption of compressed air was to a certain degree resolved (refer to Fig. 6), and the critical distance was corrected a bit up to $L^*=177.8\text{mm}$ (refer to Fig. 7). This is consistent with the previous result in that the flow is not regular in the downstream after the critical distance. The speed at the exit of the acceleration tube was greater than the speed at the critical distance L^* and, thereafter the flow was unstable.

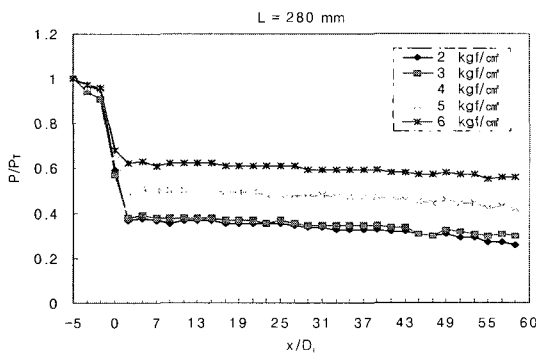


Fig. 7 Distribution of static pressure on wall surface along x -axis ($D_i=3\text{mm}$)

Likewise the choking point was shortened in the Mach number M (refer to Fig. 8), and the improvement of efficiency fell below what was expected. This study confirms that the critical distance is reduced in accordance with the decrease of the inner diameter due to the increase of friction in the tube.

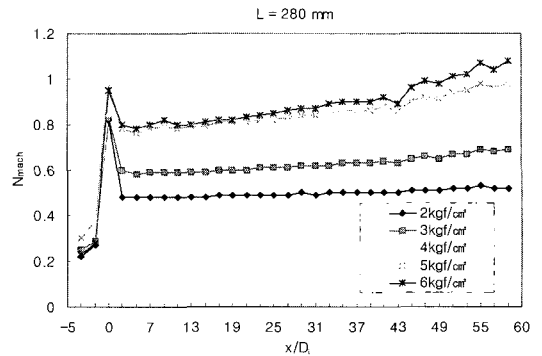


Fig. 8 Distribution of Mach number along x -axis ($D_i=3\text{mm}$)

4.2 Comparison of straight-tube type pipe and Laval-tube type pipe

Inspection of the studies by Uno and others state that the straight-tube type was much better in efficiency than the laval-tube type. Nevertheless, it was also pointed out that the angle of laval (θ) was too large and the relative length of the laval-tube was too short, and these problems should be resolved. Our step to resolve this problem is as follows. We carried out experiments with four configurations: more exactly, the entrance inner diameter $D_i=3\text{mm}$ of the acceleration tube, the exit inner diameter $D_o=4\text{mm}$ of the acceleration tube, and the acceleration tube of length $L=85\sim 190\text{mm}$. The results we obtained were that the speed of compressed air increased in general about 20% and the driving force against the weft strengthened much more (refer to Fig. 9).

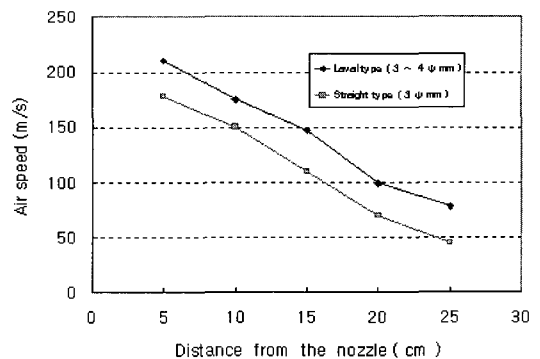


Fig. 9 Comparison of Laval-tube and Straight-type tube

As can be expected from the condition of the Fanno flow, friction increased as the flow approached toward the exit of tube. Therefore, the increase in the inner diameter is thought to minimize friction increase.

4.3 The effect of suction hole on the acceleration tube

In order to get efficient distance of weft, a suction hole has been drilled at the entrance of the acceleration tube, and this was considered to be a strategy to overcome the flow instability after the critical distance.

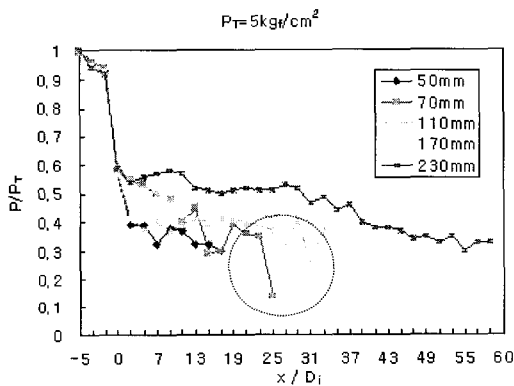


Fig.10 Distribution of static pressure on wall surface along x -axis with suction hole ($D_i = 4$ mm)

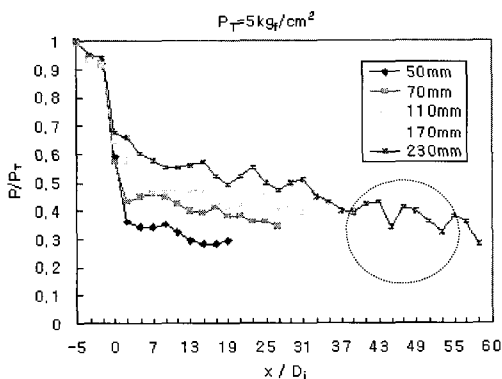


Fig.11 Distribution of static pressure on wall surface along x -axis without suction hole ($D_i = 4$ mm)

However, our results reveal that, regardless of the change in the inner diameter of the acceleration tube, the distribution of flow is stable for the case without the suction hole and for the case of short acceleration tube. Also, as can be seen from Fig. 10 and 11, the

flow is apt to be stable with increasing length of the acceleration tube up to 150mm. This is because the flow in the acceleration tube is the Fanno flow. Hence the friction increase with increasing length of the acceleration tube makes the flow approach the choking condition, and thus setting of the suction hole helps to avoid instability of the flow.

5. Conclusion

The purpose of this study was the optimum design of the air-jet nozzle for improving the capacity of an air-jet loom, and we specially analyzed the effects due to the differences of efficiency according to the change in the inner diameter of the acceleration tube and the acceleration tube type and so on. The results are as follows:

- (1) It seems better not to enlarge the tank pressure P_T and practical problems caused in the case of 4 mm diameter tube could be cured by using a 3 mm diameter tube.
- (2) The critical distance was experimentally proved to be $L^* = 195.67 (5 \text{ kg}_t/\text{cm}^2)$ for the case of $D_i = 4$ mm and $L^* = 177.8 (5 \text{ kg}_t/\text{cm}^2)$ for the case of $D_i = 3$ mm. However it seems that this difference in the critical distance has no direct relation to the improvement of the nozzle efficiency.
- (3) For the case of $D_i = 3$ mm, the compressed air is consumed less, and significant improvement is noted in the productivity. But the critical distance of the acceleration tube tends to be shorter.
- (4) Compared with the straight-tube type, the use of the Laval-tube type shows a 20% increase in the speed of compressed air as a whole, and the driving force for the weft is strengthened more.
- (5) The use of the suction hole at the exit of the acceleration tube should be decided based on the length of the acceleration tube. For the acceleration tube longer than 150mm, use of the suction hole entails an improved performance.

References

1. Ishida, T., Textile News. Jpn., Vol. 8, 1982.

2. Duxbury, V., Lord, P. and Vaswani, T., J. Textile Inst., Vol. 50, No. 558, 1959.
3. Salama, M., Adanur, S. and Mohamed, M. H., Textile Res. J., Vol. 57, No. 44, 1987.
4. Matsumoto., "A Study on the Flow Characteristics in Coaxial Jets (Part 1, Air - Experiment of Air Coaxial Jets)," JSME Vol. 38, No.311, pp. 1753-1761, 1972.
5. Kwan, A. S. H. and Ko, N.W.M., "Coherent Structure in Subsonic Coaxial Jets," J. Sound Vib., Vol. 48, pp. 203-210, 1976.
6. Champagne, F. H. and Wygnarski, I. J., "An experimental Investigation of Coaxial Turbulent Jets," Int. J. Heat Mass Transfer, Vol. 14, pp. 1445-1452, 1971.
7. Williams, T. J., Ali, M. R. M. H., and Anderson, J. "Noise and Flow Characteristics of Coaxial Jets," J. Mech. Eng. Sci., Vol. 11, pp.133-142, 1969.